# Probing chiral symmetry of nucleon by threshold $\eta\pi$ production

Daisuke Jido

*Department of Physics, Kyoto University, Kyoto 606-8502 Japan*

Makoto Oka

*Department of Physics, Tokyo Institute of Technology, Meguro, Tokyo 152-8551 Japan*

and

Atsushi Hosaka

*Numazu College of Technology, Numazu 410-8501, Japan*

**Abstract**

Double meson production of the eta and pion at the threshold region is investigated in order to determine chiral property of the nucleon. The eta can be used as a probe for the negative parity nucleon $N^* \equiv N^*(1535)$ produced in the intermediate state. The coupling of the low energy pion in the final state is then used to extract the sign of the Yukawa coupling, $g_{\pi N^* N^*}$, which distinguishes the two realizations of chiral symmetry, either naive or mirror, for the nucleon.

# 1 Introduction

Chiral symmetry with spontaneous breakdown is one of the important concepts in the dynamics of the strong interaction [1]. In QCD chiral symmetry is realized as the symmetry in light flavors, $SU(N_f)_L \times SU(N_f)_R$ for left- and right-handed quarks. Physical particles are then classified into appropriate representations of the chiral group which involve positive and negative parity states. For instance the pion and sigma can be assigned as members of the $(1/2, 1/2)$ representation, and $\rho$ and $a_1$ as the $(1, 0)+(0, 1)$ representation. These particles are then expected to be degenerate when chiral symmetry is restored.

Chiral symmetry is realized at the hadronic level either in the nonlinear or in the linear representations. The former is the basis of the chiral perturbation theory [2], and is under well control to describe dynamics of mesons and baryons at low energy as the lagrangian is expanded in powers of small momenta. The latter embodies the spontaneous breakdown of chiral symmetry. Therefore, it is suited to the study of the change in the vacuum toward the restoration of chiral symmetry. However, such a study, by regarding baryons explicitly as representations of chiral symmetry, has been performed only by a limited number of authors [3, 4, 5]. In previous publications [6, 7, 8], we have pointed out that there are two classes of linear representations for baryons when there are positive and negative parity baryons. We have called the one naive and the other mirror assignments [7, 10]. Physical implications of these two assignments are very different [7, 8, 9]. In the naive assignment, the positive and negative parity nucleons belong to different chiral multiplets, and therefore, chiral symmetry does not relate them. In contrast, in the mirror assignment, they belong to the same chiral multiplet, where several nontrivial features emerge. For instance nucleon masses can remain finite when chiral symmetry is restored, which is a feature that can not be possible in the naive assignment.

The mirror assignment was first considered in literatures by Lee [3] and later discussed by DeTar and Kunihiro [4] in some detail. Also an interesting suggestion was made recently by Jido, Kunihiro and Hatsuda [11], where nucleon and delta resonances are put in the mirror chiral multiplet. There, observed masses and decay strengths are remarkably consistent with predictions of a simple linear sigma model. Nevertheless, so far, we can not clearly distinguish these chiral assignments in physical nucleons, since observations for key quantities are rather difficult.

One thing which differs in the two chiral assignments is the relative sign of the axial charges ($g_A$ and $g_A^*$), or equivalently the pion coupling ($g_{\pi NN}$ and $g_{\pi N^* N^*}$) for the positive and negative parity nucleons. The difference in the sign may be observed through interference effects. The purpose of the present paper is to propose one of such processes, which we hope will be performed in future experiments.

If we assume that the relevant negative parity nucleon is $N(1535)$, the first excited state of negative parity, it can be probed by the production of the eta meson. Therefore,

we are lead naturally to the study of the $\pi\eta$ production especially at the threshold region. As an illustration, we investigate in this paper a pion induced process, $\pi^- + p \to \pi^- + \eta + p$. This reaction would be relatively in easy access by experiments, since the charged particles ($\pi^-$ and $p$) are present and therefore the $\eta$ in the final state can be observed by invariant mass analysis of the $\pi^- p$ system.

The contents of this paper are the followings. In the next section we briefly review the chiral symmetry for the nucleon. The physical consequences of the naive and mirror assignments are summarized. In section 3, we formulate the two meson productions of the pion and eta at the threshold region. In section 4, we present several kinds of cross sections and discuss how the two assignments differ in various observed quantities. Conclusion is given in section 5.

# 2 Chiral symmetry of the nucleon

Let us start with a brief review on chiral representations of the nucleon [8]. To be specific, we consider the chiral group with two flavors, $SU(2)_L \times SU(2)_R$. The nucleon field $N$ is decomposed into the left and right handed components, $N = N_l + N_r$. Assuming linear representations of the chiral group for the nucleon, $N_l$ and $N_r$ form the two fundamental representations of the chiral group, $(1/2, 0)$ and $(0, 1/2)$, respectively, where the first (second) number in the parentheses refers to the representation of $SU(2)_L$ ($SU(2)_R$). Chiral transformations are isospin transformations for the left and right handed nucleons as $N_l \to g_L N_l$ and $N_r \to g_R N_r$, where $g_L \in SU(2)_L$ and $g_R \in SU(2)_R$. Hence, the transformation on the left- or right-handed nucleon is called the left ($L$) or right ($R$) chiral transformation. For a massive nucleon, the mass term must couple the left and right handed components (the Dirac mass term) as $m\bar{N}N = m(\bar{N}_l N_r + \bar{N}_r N_l)$. Hence chiral symmetry must be broken.

When there are two different nucleon fields the situation can change. Let us denote the two nucleons as $N^+$ and $N^-$. Then we can introduce two different ways of chiral assignments for the left and right handed components, as shown in Table 1. Here the superscripts $+$ and $-$ imply the parity of the two nucleons. In the naive assignment, the left- and right-handed components of the two nucleons, $N^+$ and $N^-$, behave in the same way, while in the mirror assignment, the roles of the left- and right-handed components of the second nucleon $N^-$ are interchanged, just as in the mirror world where the left and right hand sides are interchanged. The reason that such an assignment is possible is that the chiral symmetry is an internal symmetry and when there are two (or generally more) different nucleon fields, the left and right handed components of different nucleons do not necessarily behave in the same way. In the mirror assignment, due to the opposite transformation property, the chiral invariant mass term is allowed,

Table 1: Two chiral assignments for two nucleons.

| Naive | | | | Mirror | | | |
|---|---|---|---|---|---|---|---|
| $N_l^+$ | $N_l^-$ | $N_r^+$ | $N_r^-$ | $N_l^+$ | $N_r^-$ | $N_r^+$ | $N_l^-$ |
| (1/2,0) | | (0,1/2) | | (1/2,0) | | (0,1/2) | |

$m(\bar{N}^+\gamma_5 N^- - \bar{N}^-\gamma_5 N^+) = m(\bar{N}_l^+ N_r^- + \bar{N}_r^- N_l^+ - \bar{N}_l^- N_r^+ - \bar{N}_r^+ N_l^-)$.

In our previous publication, based on these classifications, we have investigated several physical implications of the two assignments using linear sigma models [8, 9]. Main results are summarized in Table 2. The masses of the nucleons in the Wigner phase should be absent in the naive case, while they can be finite in the mirror case. It would be interesting to study physics near the chiral phase transition. The $\pi NN^*$ coupling in the chiral limit should vanish at the tree level in the naive assignment, which is qualitatively supported by the small observed value, $g_{\pi NN^*} \sim 1$. The off-diagonal axial charge $g_A^{NN^*}$ at finite temperature and/or density should be suppressed in the naive case, while enhanced in the mirror case, as compared to that at the normal vacuum. This is because $g_A^{N^*N^*}$ should approach one in the naive case, while zero in the mirror case, as the broken chiral symmetry tends to be restored.

In the present work, among various properties listed there, we would like to discuss a possibility to measure the sign of the axial charge which is perhaps the most clearcut signal to distinguish the two chiral assignments. The sign of the axial charges, when combined with the Goldberger-Treimann relation, can be turned into the sign of the Yukawa couplings. Then the difference in the sign of the couplings $g_{\pi N^+N^+}$ and $g_{\pi N^-N^-}$ could be observed in a suitable hadronic processes which involve the pion.

In the following discussion we assume that candidates of the two nucleons are the ground state nucleon $N(938)$ and the first negative parity excited state $N(1535)$. It is known that $N(1535)$ couples strongly to the eta meson, which can be used as an indication that $N(1535)$ is produced in relevant reactions. In what follows we often denote $N(939)$ simply by $N$, and $N(1535)$ by $N^*$.

# 3 Formulation

We investigate an eta pi production process $\pi^- + p \to \pi^- + \eta + p$, in order to extract the relative sign of $g_{\pi N^*N^*}$ to $g_{\pi NN}$. As indicated in introduction, our basic idea is to see interference effects due to sign difference between the two coupling constants, $g_{\pi NN}$ and $g_{\pi N^*N^*}$. Let us see the diagrams (1) and (2) in Figs.1. The $\pi NN$ coupling is in the diagram (1), while the $\pi N^*N^*$ coupling in the diagram (2). The relative sign of the couplings results in either constructive or destructive sum of these two diagram.

Table 2: Comparison between the naive and mirror assignments.

| | Naive assignment | Mirror assignment |
|---|---|---|
| Chiral multiplet | $(N^+, \gamma_5 N^+)$ and $(N^-, \gamma_5 N^-)$ | $(N^+, \gamma_5 N^+, N^-, \gamma_5 N^-)$ |
| | $N^+$ and $N^-$ are independent | |
| Mass in the Wigner phase | 0 | $m_0$ (finite) |
| $\pi N N^*$ coupling | 0 | $(a+b)/\cosh\delta$ |
| Relative sign of $g_A^{NN}$ and $g_A^{N^*N^*}$ | Positive | Negative |
| $g_{\pi NN}(\rho, T)$ | Decrease | Decrease |
| $g_{\pi NN^*}(\rho, T)$ | Increase | Decrease |

Our assumptions are the followings

1. Resonance ($N(1535)$) pole dominance. This is considered to be good particularly for the $\eta$ production process at the threshold region.
2. The $\eta$ meson couples only through $N(1535)$. It is known that the $\eta$ meson couples only weakly with the nucleon and other resonances.
3. Pions are inserted in all possible ways to the diagrams.

Under these assumptions, we can write six diagrams as shown in Figs. 1.

For meson nucleon interactions, we take the interaction lagrangians:

$$\begin{aligned} L_{\pi NN} &= g_{\pi NN} \bar{N} i\gamma_5 \vec{\tau} \cdot \vec{\pi} N \,, \\ L_{\eta NN^*} &= g_{\eta NN^*} (\bar{N} \eta N^* + \bar{N}^* \eta N) \,, \\ L_{\pi NN^*} &= g_{\pi NN^*} (\bar{N} \tau \cdot \pi N^* + \bar{N}^* \tau \cdot \pi N) \,, \\ L_{\pi N^* N^*} &= g_{\pi N^* N^*} (\bar{N}^* i\gamma_5 \tau \cdot \pi N^*) \,. \end{aligned} \tag{1}$$

Here we have adopted pseudo-scalar couplings which arise naturally in linear sigma models. We use these interactions both for the naive and mirror cases with empirical coupling constants for $g_{\pi NN} \sim 10$, $g_{\pi NN^*} \sim 0.7$ and $g_{\eta NN^*} \sim 2$. The second and third are determined from the partial decay widths, $\Gamma_{N^*(1535)\to\pi N} \approx \Gamma_{N^*(1535)\to\eta N} \sim 70$ MeV [12], although large uncertainties for the width have been reported [13, 14]. The unknown parameter is the $g_{\pi N^* N^*}$ coupling. One can estimate it by using the theoretical value of the axial charge $g_A^*$ and the Goldberger-Treimann relation for $N^*$. When $g_A^* = \pm 1$ for the naive and mirror assignments, we find $g_{\pi N^* N^*} = g_A^* m_{N^*}/f_\pi \sim \pm 15$. Here, just for simplicity, we use the same absolute value as $g_{\pi NN}$. The coupling values used in our computations are summarized in Table 3.

Besides the resonance pole contributions as shown in Fig. 1, there are several other possible terms. We ignore all of them from the following reasons.

- **Background:**

  We can consider three diagrams as shown in Figs. 2 (a-c). All of them are not allowed

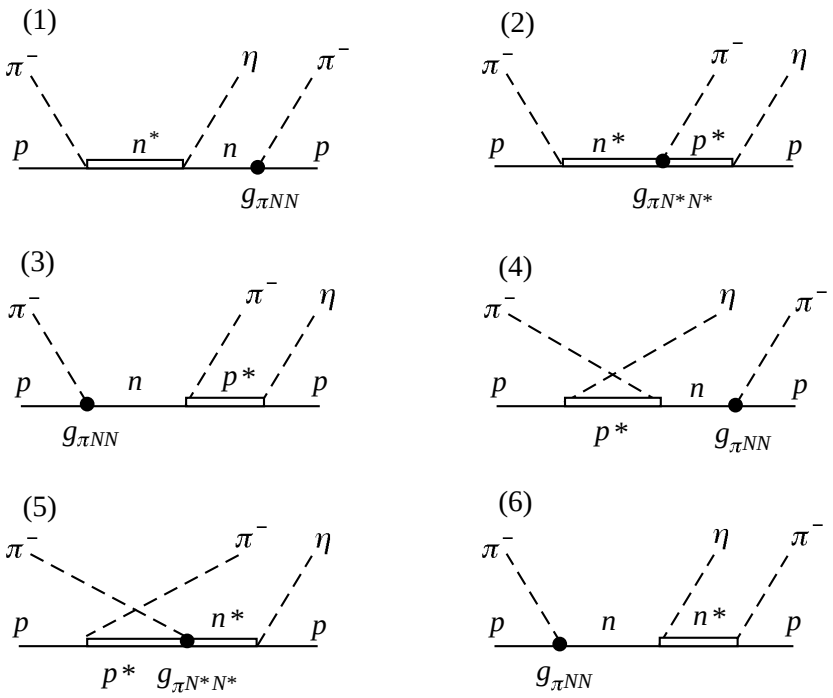


Figure 1: Six pole dominant diagrams for $\eta\pi$ production.

Table 3: Parameters used in our calculation.

| $m_N$ | $m_{N^*}$ | $\Gamma_{N^*}$ | $g_{\pi NN}$ | $g_{\pi NN^*}$ | $g_{\eta NN^*}$ | $g_{\pi N^* N^*}$ |
|---|---|---|---|---|---|---|
| 938 | 1535 | 140 | 13 | 0.7 | 2.0 | 13 (naive) |
| (MeV) | (MeV) | (MeV) | | | | –13 (mirror) |

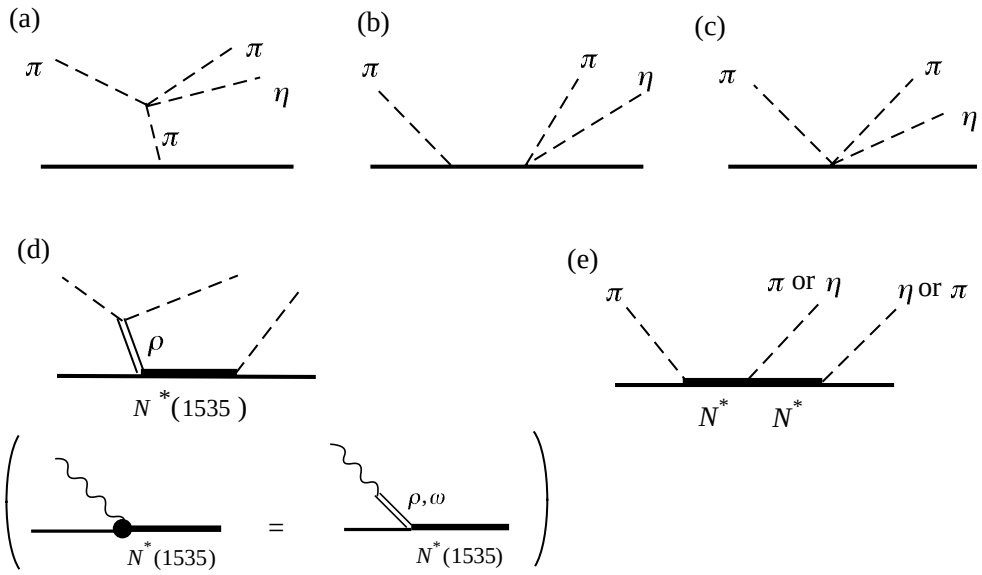


Figure 2: Various contributions to $\pi N \to \eta\pi N$.

due to G-parity. For (a), the vertex $\pi\pi\pi\eta$ is G-parity forbidden, since $G(\pi) = -1$ and $G(\eta) = 1$. For (b) and (c), to estimate the diagrams, we first consider the lowest order of the chiral expansion in the Lagrangian [15]. For two-meson nucleon vertices in (b), the two mesons are correlated as vector mesons (such as $\rho$) which have G-parity plus. Therefore, the G-parity minus combination $\pi\eta$ is not allowed. Similarly, three meson vertices in (c) have axial vector correlation with negative G-parity, and hence the positive G-parity combination $\pi\pi\eta$ is not possible. These selection rules are explicitly satisfied in actual chiral lagrangians.

- $\rho$ **meson:**

  We have computed the diagram in Fig. 2 (d) explicitly. The rho meson coupling to $N$ and $N^*$ is extracted from the helicity amplitudes $A_{1/2} \sim 0.08\ GeV^{-1/2}$ [12] using the vector meson dominance as shown in Fig. 2 (d). It turns out that the contribution to the cross section is negligibly small as compared to the resonance pole terms in Fig. 1 by about factor $10^{-3}$.

- **Off diagonal couplings:**

  Finally, one would expect contributions where two resonances appear in intermediate states as shown in Fig. 2 (e). Again we can ignore these diagrams safely, since there is no strong indication that any resonances couples to $N^*(1535)$ by emitting a pion [12]. In particular, the delta resonance which could be excited strongly by the incident pion does not couple to $N^*(1535)$, since the observed branching ratio of $N^*(1535) \to \Delta\pi$ is less than 10 %.

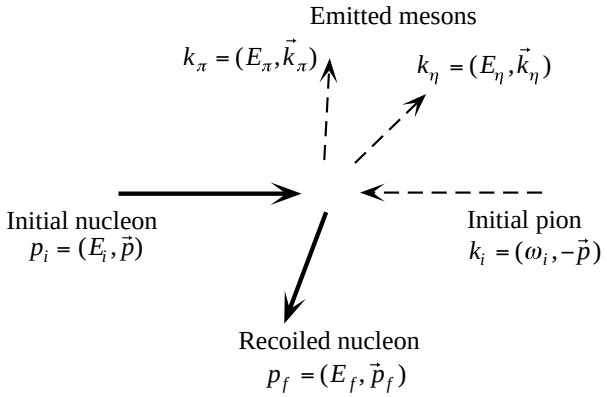


Figure 3: Definition of momentum variables.

Now the $S$-matrix is computed using the reduction formula

$$\begin{aligned} S_{fi} &= {}_{out}\langle p_f, k_\pi, k_\eta | k_i, p_i \rangle_{in} \\ &= disc. + (iZ_\pi^{-1/2})^2 (iZ_\eta^{-1/2}) \int d^4x d^4y d^4z \, e^{ik_\pi x + ik_\eta y - ik_i z} \\ &\quad (\Box_x + m_\pi^2)(\Box_y + m_\eta^2)(\Box_z + m_\pi^2) {}_{out}\langle p_f | T(\pi^i(x)\eta(y)\pi^j(z)) | p_i \rangle_{in} \,. \end{aligned} \tag{2}$$

The momentum variables are defined as in Fig. 3.

In the perturbation theory, the matrix element can be computed as

$$\begin{aligned} &{}_{out}\langle p_f | T(\pi^i(x)\eta(y)\pi^j(z)) | p_i \rangle_{in} \\ &= i^3 \langle p_f | T(\pi^i(x)\eta(y)\pi^j(z) \int d^4x_1 d^4x_2 d^4x_3 L_{\eta NN^*}(x_1) L_{\pi NN^*}(x_2) \\ &\qquad \times (L_{\pi NN}(x_3) + L_{\pi N^* N^*}(x_3))) | p_i \rangle_{in} \,. \end{aligned} \tag{3}$$

After taking the Wick contraction in (3) which is then inserted in (2), we find an ordinary expression for amplitudes in momentum space. For instance the amplitudes for Fig. 1 (1) and (2) are given by

$$T(1) = \bar{u}(p_f) \frac{(i\sqrt{2} g_{\pi NN} i\gamma_5) i(i g_{\eta NN^*}) i(i\sqrt{2} g_{\pi NN^*})}{(\not{p}_f + \not{k}_\pi - m_N)(\not{p}_i + \not{k}_i - m_{N^*} + \frac{i}{2}\Gamma)} u(p_i) \,, \tag{4}$$

$$T(2) = \bar{u}(p_f) \frac{(i g_{\eta NN^*}) i(i\sqrt{2} g_{\pi N^* N^*} i\gamma_5) i(i\sqrt{2} g_{\pi NN^*})}{(\not{p}_f + \not{k}_\eta - m_{N^*} + \frac{i}{2}\Gamma)(\not{p}_i + \not{k}_i - m_{N^*} + \frac{i}{2}\Gamma)} u(p_i) \,, \tag{5}$$

where $u$'s are the Dirac spinors for the nucleon.

Using these $\mathcal{T}$ matrices, we calculate cross section as

$$d\sigma = \frac{2m_N}{4\sqrt{(p_i \cdot k_i)^2 - m_N^2 m_\pi^2}} \frac{1}{2} \sum_{spin} |\mathcal{T}_{fi}|^2 d\Phi \,, \tag{6}$$

where the phase space of the three body final state is given by

$$d\Phi = (2\pi)^4 \delta(p_i + k_i - p_f - k_\pi - k_\eta) \frac{d^3k_\pi}{(2\pi)^3 2E_\pi} \frac{d^3k_\eta}{(2\pi)^3 2E_\eta} \frac{m_N d^3p_f}{(2\pi)^3 E_f} \,. \tag{7}$$

Here the convention for the normalization is

$$\bar{u}^{(\alpha)}(p)u^{(\beta)}(p) = \delta^{\alpha\beta}\,, \tag{8}$$

$$\langle p|p'\rangle = \frac{E}{m}(2\pi)^3\delta^3(\vec{p}-\vec{p}')\,. \tag{9}$$

In the center of mass frame, the phase space integral reduces to

$$d\Phi = \frac{m_N}{4(2\pi)^5}dE_\pi dE_f d\alpha d(\cos\beta)d\gamma\,. \tag{10}$$

In the center of mass frame, the momenta of the emitted particles, $\vec{p}_f$ $\vec{k}_\pi$ and $\vec{k}_\eta$, lie in a plane. If the energies of the proton and the pion in the final state, $E_f$, $E_\pi$ are fixed, then the relative angles between either two of $\vec{p}_f$, $\vec{k}_\pi$ and $\vec{k}_\eta$ can be determined. Therefore, the orientations of the three momenta are specified by the three Euler angles $\alpha$, $\beta$ and $\gamma$.

We have computed the integral over the three body phase space in the Monte Carlo method. The number of configurations is taken more than 30,000, depending on the kinds of cross sections. The total cross section is computed in a schematic way as

$$\begin{aligned}\sigma &= (\text{K.F.})\int|\mathcal{T}(\xi)|^2 d\Phi \\ &\to (\text{K.F.})\frac{1}{N}\sum_{i=1}^{N}|\mathcal{T}(\xi_i)|^2 V\,,\end{aligned} \tag{11}$$

where $\xi = (E_f, E_\pi, \alpha, \cos\beta, \gamma)$. The volume of the phase space is given by the integral

$$V = \frac{m_N}{4(2\pi)^5}4\pi^2\int_{E_{min}}^{E_{max}}\frac{2\sqrt{(E_\eta^{*2}-m_\eta^2)(E_\pi^{*2}-m_\pi^2)}}{E_{cm}}dE_\pi\,, \tag{12}$$

where $E_\eta^*$ and $E_\pi^*$ are the energies of the emitted $\eta$ and $\pi$ in the rest frame of the emitted nucleon and eta. They are

$$E_\eta^* = \frac{E_{cm}^2 - m_N^2 + m_\eta^2 + m_\pi^2 - 2E_{cm}E_\pi}{2\sqrt{E_{cm}^2 + m_\pi^2 - 2E_{cm}E_\pi}}\,, \tag{13}$$

$$E_\pi^* = \frac{E_{cm}E_\pi - m_\pi^2}{\sqrt{E_{cm}^2 + m_\pi^2 - 2E_{cm}E_\pi}}\,. \tag{14}$$

The lower and upper bounds of the integral (12) are given by

$$E_{min} = m_\pi\,, \tag{15}$$

$$E_{max} = \frac{E_{cm}^2 + m_N^2 - (m_N+m_\eta)^2}{2E_{cm}}\,. \tag{16}$$

To compute differential cross section $d\sigma(\zeta)$ where $\zeta$ is a representative of the variable we need, for instance the angle of the emitted pion in the center of mass frame and the momentum of the emitted pion in the laboratory frame, we put a delta function of finite range $\Delta\zeta$ in the integrand of the total cross section.

$$\begin{aligned}d\sigma(\zeta) &= (\text{K.F.})\int|\mathcal{T}(\xi)|^2\delta(\zeta'(\xi)-\zeta)d\Phi \\ &\to (\text{K.F.})\frac{1}{N}\sum_{i=1}^{N}|\mathcal{T}(\xi_i)|^2\frac{\sqrt{\pi}}{\Delta\zeta^2}e^{-\frac{(\zeta'(\xi_i)-\zeta)^2}{\Delta\zeta^2}}V\,.\end{aligned} \tag{17}$$

Note that the phase space is represented in the center of mass frame. The $\zeta'$ stands for the translation of the variables $\xi$. For example, $\zeta'$ is a boost transformation from the CM frame to the laboratory frame to calculate the differential cross section in the laboratory frame.

# 4 Results and discussions

The total cross sections is shown in Fig. 4 as functions of the energy of the initial pion for the naive and mirror cases. The difference between the two is due to the sign of the $g_{\pi N^* N^*}$ coupling. The cross sections increase, as the initial pion energy and correspondingly the phase space of the final three body state increase. For $P_{cm} \gtrsim P_{cm}^{\rm thresold} + 50$ MeV/c ($P_{cm}^{\rm threshold} = 528$ MeV/c), the cross sections reach more than ten micro barn, which will be experimentally accessible. In the whole energy region as shown in Fig. 4 the cross section is larger in the mirror model, which is about twice as that in the naive model.

Among various terms shown in Fig. 1, major contributions are from the diagrams (2) and (3). In Fig. 5, we show relative strengths of $|T(2)|^2$, $|T(3)|^2$ and their interference $2T(2)^* T(3)$ in the naive assignment. The difference between the naive and mirror assignments in the total cross section is from the sign difference of this term. The third major contribution is from $T(1)$ which is also shown there. Other terms are negligible.

The term $T(3)$ gives a large contribution to the cross section as compared with $T(1)$ and $T(2)$, although we expect naively that the terms $T(1)$ and $T(2)$ are the dominant contribution with considering of their energy denominators. This is so because of the p-wave nature of the $\pi NN$ coupling at the initial state of the diagram 3. The $\pi NN$ and $\pi N^* N^*$ are reduced to the p-wave couplings in the non-relativistic limit. Near the threshold the emitted pion has a comparably small momentum. In the diagram 1 and 2 the p-wave coupling is attached on the emitted pion. Therefore it gives a suppression to their contributions, while in the diagram 3 the p-wave coupling is on the initial pion, which has a larger momentum than the emitted pion.

The total cross section alone is not sufficient to distinguish the difference between the naive and mirror assignments, because it is hard to determine the absolute values of the cross section in experiments and there are the unknown parameter $g_{\pi N^* N^*}$. Therefore some qualitative differences are desired. Then let us discuss differential cross sections.

- **Angular distributions:** In Fig. 6, we show angular distributions of the final state pion in the center of mass frame. This shows the clear difference between the two models. This comes from the p-wave nature of the $\pi N^* N^*$ coupling in the diagram 2. As it is mentioned before, the main contributions are given by the diagram 2 and 3, and difference by the sign of $g_{\pi N^* N^*}$ appears in the sign of the interference of $T(2)$ and $T(3)$. The first nucleon in the intermediate state is rest in the center of mass

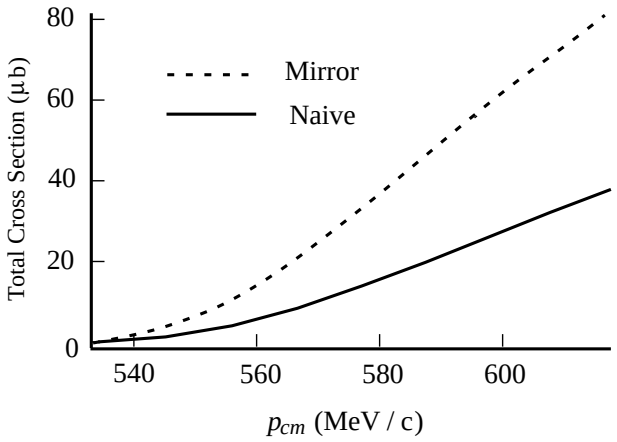


Figure 4: Total cross sections of $\pi^- p \to \eta\pi^- p$ for the naive and mirror models as functions of the initial pion momentum $P_{c.m.}$ in the center of mass frame.

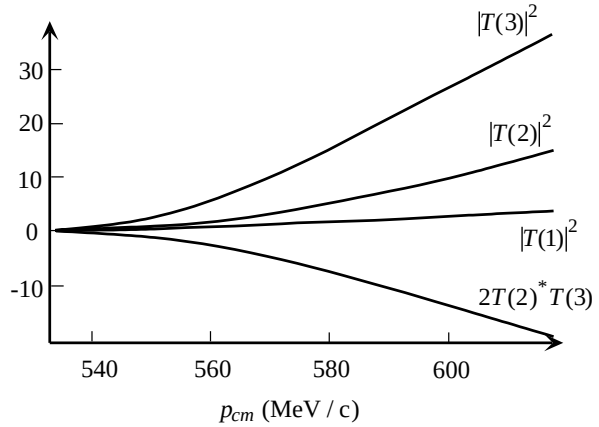


Figure 5: Separate contributions from various terms of Fig. 1. The amplitude of the cross term $2T(2)^*T(3)$ corresponds to the naive assignment. It changes the sign for the mirror assignment.

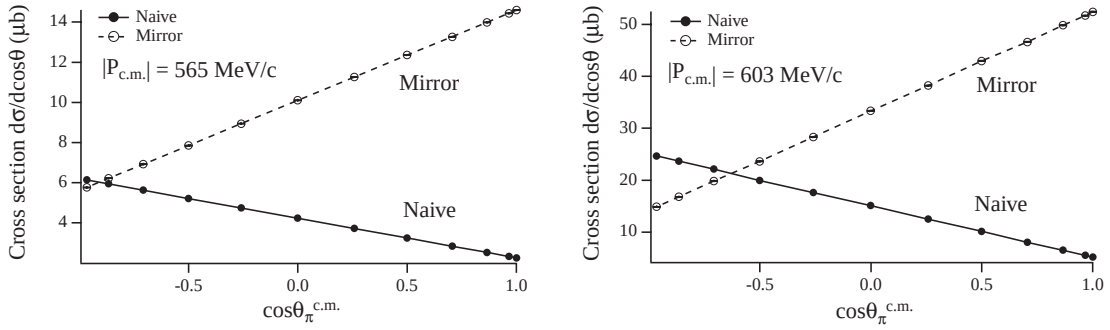


Figure 6: Angular distributions of the $\pi^-$ in the final state.

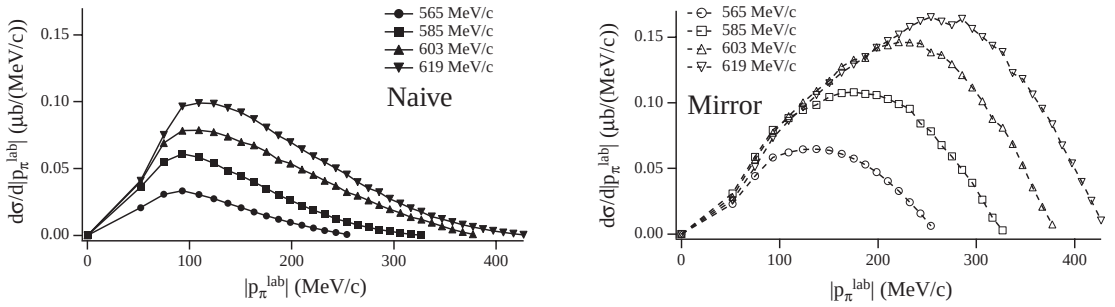


Figure 7: Momentum distributions of the $\pi^-$ in the final state.

frame. Due to the structure of the Yukawa vertex, the emitted pion in the diagram 2 is in p-state, which gives monotonic increase or decrease in the differential cross sections as functions of $\cos\theta_\pi^{c.m.}$. On the other hand, the emitted pion in the diagram 3 is in s-wave, which has no angular distributions. Therefore the cross term of $T(2)$ and $T(3)$ behaves linearly in $\cos\theta_\pi^{c.m.}$, and the apparently different behaviors in the $\cos\theta_\pi^{c.m.}$ dependence is due to the difference in the sign of the coupling $g_{\pi N^* N^*}$. This angular dependence would be one of the cleanest observables to distinguish the naive or mirror assignments.

- **Momentum distributions:** Another example which is useful is the momentum (energy) distribution of one of the final state particles. We plot the momentum distribution of the emitted pion in the laboratory frame in Fig. 7 for several incident energies. What differs in the two chiral assignments is the position of the peak in the cross sections. In the naive case, it does not depend on the incident energy, while in the mirror case, it shifts to higher momentum region as the incident energy is increased.

# 5 Conclusions

We have proposed the two meson production reaction $\pi^- p \to \pi^- \eta p$ to probe the chiral symmetry for the nucleon. Since chiral symmetry plays essential roles in hadron physics, its manifestation in the baryon sector as well as in the meson sector is very important to understand the nature of the QCD vacuum. Our aim is to extract the relative sign of the two strong coupling constants, $g_{\pi NN}$ and $g_{\pi N^* N^*}$ through their interference, since it is a signal to distinguish the chiral representations of the nucleons.

We have investigated various cross sections for $\pi^- p \to \pi^- p \eta$. Having in mind possible experimental setups we have shown total cross sections, angular distributions of the pion and energy distributions of the pion. In fact, we have also computed differential cross sections as functions of the final proton angles and momenta. However, we did not see very clear distinction between the naive and mirror chiral assignments. The three examples we have presented here, the total cross section, angular and momentum distributions of the emitted pion, are the processes which show the most visible difference in the two assignments.

In addition to the reaction we have considered in the present paper, there are similar ones such as $\pi^+ p \to \pi^+ \eta p$, $\gamma p \to \pi^0 \eta p$, and so on. In the former, as the total isospin is $I = 3/2$, the $\Delta(1232)$ channel would be dominant and therefore, interference effects among various terms may not be expected. In the latter, the final state contains two neutral particles ($\eta$ and $\pi^0$) involved, which makes experimental setup difficult.

Theoretical predictions have been made under the assumption of resonance dominance of $N^*(1535)$. The unique feature of the resonance which strongly couples to $\eta$ makes the present theoretical analysis rather simple, since $\eta$ can filter only a limited number of diagrams. Perhaps, the physical as well as practical (experimental) conditions select almost uniquely the present reaction as the most convenient one.

We have then shown that various cross sections differ significantly depending on whether the nucleons belong to the naive or mirror chiral assignments. Not only a single but also several observations for different quantities will be useful to obtain information on the chiral symmetry for the nucleon.

# Acknowledgments

We acknowledge H. Kim and M. Iwasaki for discussions. This work is supported in part by the Grant-in-Aid for scientific research (C)(2) 11640261.

# References

[1] S. Coleman, *Aspects of Symmetry*, Cambrige University Press, Cambrige (1985).

[2] J. Gasser and H. Leutwyler, Nucl. Phys. B250 (1985) 465; U.-G. Meissner, Rep. Prog. Phys. 56 (1993) 903; A. Pich, Rep. Prog. Phys. 58 (1995) 563; G. Ecker, Prog. Part. Nucl. Phys. 35 (1995) 1.

[3] B. W. Lee, *Chiral Dynamics*, Gordon and Breach, New York, (1972)

[4] C. DeTar and T. Kunihiro, *Phys. Rev.* D **39**, 2805 (1989).

[5] T.D. Cohen and X. Ji, *Phys. Rev.* D **55**, 6870 (1997)

[6] D. Jido, M. Oka and A. Hosaka, *Phys. Rev. Lett.* **80**, 448 (1998)

[7] Y. Nemoto, D.Jido, M. Oka and A. Hosaka, *Phys. Rev.* D **57**, 4124 (1998).

[8] D.Jido, Y. Nemoto, M. Oka and A. Hosaka, *Nucl. Phys.* A **671**, 471 (2000).

[9] H. Kim, D.Jido, and M. Oka, *Nucl. Phys.* A **640**, 77 (1998).

[10] The term "mirror fermion" is introduced in the paper; J. Maalampi and M. Roos, Phys. Rep. **186**,53 (1990)

[11] D. Jido, T. Kunihiro and T. Hatsuda, *Phys. Rev. Lett.* **84**, 3252 (2000).

[12] C. Caso et al. (Particle Data Group), Euro. Phys. J. C3 (1998) 1

[13] D.M. Manley and E.M. Salesky, *Phys. Rev.* D **45**, 4002 (1992).

[14] T.P. Vrana, S/A. Dytman and T.-S.H. Lee, Phys. Reports 328, 181 (2000).

[15] See, for instance, J.F. Donoghue, E. Golowich and B.R. Holstein, *Dynamics of the standard model*, Cambridge monographs on particle physics (1992).